ELSEVIER

Journal of Nuclear Materials 281 (2000) 129–139

journal of nuclear materials

www.elsevier.nl/locate/jnucmat

Kinetics of thermal decomposition of $Th(C_2O_4)_2 \cdot 6H_2O$

Kitheri Joseph, R. Sridharan, T. Gnanasekaran *

Materials Chemistry Division, Chemical Group, Indira Gandhi Centre for Atomic Research, Kalpakkam, Tamil Nadu 603102, India

Received 28 February 2000; accepted 5 July 2000

Abstract

Thermal decomposition of thorium oxalate hexahydrate was investigated under nonisothermal and isothermal conditions in moist argon by using simultaneous thermogravimetric–differential thermal analyser. Nonisothermal experiments were carried out at various linear heating rates. Intermediates formed in each stage of the thermal decomposition of thorium oxalate hexahydrate were deduced. Kinetics of decomposition in each stage were evaluated from the dynamic TGA–DTA data by means of Coats and Redfern equation. The values of the activation energy (E) and the pre-exponential factor (A) of each stage of the thermal decomposition at various linear heating rates were calculated. These kinetic parameters were evaluated from isothermal experiments also and probable decomposition mechanism is proposed.

1. Introduction

Thoria is generally produced by a process involving calcination of thorium oxalate. Although several studies have been carried out on the decomposition of thorium oxalate and its hydrates [1–5], there is disagreement regarding the nature of the intermediates formed during the decomposition and in decomposition temperatures. Kinetic parameters for all the decomposition stages have also not been reported so far. In the present work, experiments were carried out to deduce the decomposition pattern of thorium oxalate hexahydrate under well-controlled conditions by TGA–DTA techniques. Kinetic parameters for different decomposition stages are derived from the results and conclusions drawn from them are presented.

2. Literature data on decomposition of thorium oxalates

Thorium oxalate is known to form three hydrates, namely mono-, di-, and hexahydrates. In addition to these hydrates, possible existence of thorium oxalate pentahydrate was proposed earlier [1]. When precipitation from an aqueous solution is adopted for preparation of thorium oxalate, it is obtained in hexahydrate form. In some of the earlier works, drying of samples at some stage of preparation could have resulted in formation of a mixture of hydrates leading to the proposal of pentahydrate.

Decomposition of hydrates of thorium oxalates are reported in [1–5]. D'Eye and Sellman [1], Padmanabhan et al. [2] and Aybers [5] employed dihydrates as their starting oxalate, while Wendlandt et al. [3] and Subramanian et al. [4] used hexahydrate. Salient aspects of these studies are summarised in Table 1. It is seen from the table that D'Eye and Sellman, Wendlandt et al. and Subramanian et al. have not reported the formation of thorium oxalate monohydrate during the decomposition process, whereas the other two groups of workers have deduced the formation of this compound as the intermediate. D'Eye and Sellman reported formation of carbonate as intermediate in the decomposition process while Aybers proposed formation of carbonate and oxycarbonate as intermediates. Further, the decomposition temperature of dihydrate to form the monohydrate reported in [2,5] are widely different. Except in the work of Aybers, the starting compounds and the different intermediate products were not characterised by other instrumental techniques. All these information emphasize the need for decomposition studies on well-characterised thorium oxalate hydrate and characterisation of intermediates in order to deduce a self-consistent sequence for the decomposition reaction.

* Corresponding author. Tel.: +91-4114 40219; fax: +91-4114 40365.

E-mail address: gnani@igcar.ernet.in (T. Gnanasekaran).

0022-3115/00/$ - see front matter
PII: S0022-3115(00)00241-5

Table 1
Literature data on thermal decomposition of thorium oxalate hydrates

Authors	Experimental technique and conditions	Reaction sequence reported	Remarks
D'Eye and Sellmann [1]	Decomposition carried out at different isothermal heating and quantitative estimation of solid residues and gases evolved. Carrier gas: dry air, N_2	$Th(C_2O_4)_2 \cdot 2H_2O \overset{543\ K}{\rightarrow} Th(C_2O_4)_2 + 2H_2O$ $Th(C_2O_4)_2 \overset{603\ K}{\rightarrow} Th(CO_3)_2 + 2CO$ $\downarrow$ $ThO_2 + 2CO_2$	Authors reportedly employed dihydrate. Samples and intermediates not structurally characterised by XRD
Padmanabhan et al. [2]	Independent TGA and DTA systems. Heating rate: 6°C/min Sample size for TG: 500 mg; Sample size for DTA: NA; Ambient: air	$Th(C_2O_4)_2 \cdot 2H_2O \overset{393\ K}{\rightarrow} Th(C_2O_4)_2 \cdot H_2O + H_2O$ $Th(C_2O_4)_2 \cdot H_2O \overset{503\ K}{\rightarrow} Th(C_2O_4)_2 + H_2O$ $Th(C_2O_4)_2 \overset{643\ K}{\rightarrow} ThO_2 + 2CO + 2CO_2$	No XRD analysis of starting compound and intermediates. Preliminary kinetic data utilising Freemann and Caroll method
Wendlandt et al. [3]	Independent TGA and DTA systems; Heating rate: 10°C/min; Sample size: 75–100 mg; Ambient: air	$Th(C_2O_4)_2 \cdot 6H_2O \overset{373\ K}{\rightarrow} Th(C_2O_4)_2 \cdot 2H_2O + 4H_2O$ $Th(C_2O_4)_2 \cdot 2H_2O \overset{523\ K}{\rightarrow} Th(C_2O_4)_2 + 2H_2O$ $Th(C_2O_4)_2 \rightarrow ThO_2 + 2CO + 2CO_2$	Onset temperatures for decompositions deduced from DTA peak in paper. No XRD analysis of samples and intermediates An endothermic peak centered at 658 K and a broad exothermic peak centered at about 833 K were reported. They were attributed to the decomposition of anhydrous thorium oxalate to thoria

Subramanian et al. [4]	DTA system Heating rate: 10°C/min; Sample size: not given; Ambient: air	$Th(C_2O_4)_2 \cdot 6H_2O \rightarrow Th(C_2O_4)_2 \cdot 2H_2O + 4H_2O$	No XRD analysis of samples and intermediates
		$Th(C_2O_4) \cdot 2H_2O \rightarrow Th(C_2O_4)_2 + 2H_2O$	
		$Th(C_2O_4)_2 \rightarrow ThO_2 + 2CO + 2CO_2$	Two endothermic peaks centered at 425 and 523 K were attributed to the first and second dehydration steps. The exothermic peak centered at 679 K was attributed to the formation of thoria
Aybers [5]	Simultaneous TGA–DTA system; Heating rate: 5°C/min; Sample size: 130 mg; Ambient: air. In addition, surface area of products measured as a function of temperature correlated to reaction sequence	$Th(C_2O_4)_2 \cdot 2H_2O \overset{453\ K}{\rightarrow} Th(C_2O_4)_2 \cdot H_2O + H_2O$	Starting oxalate i.e., $Th(C_2O_4)_2{\cdot}2H_2O$ characteristised by XRD
		$Th(C_2O_4)_2 \cdot H_2O \overset{553\ K}{\rightarrow} Th(C_2O_4)_2 + H_2O$	
		$Th(C_2O_4)_2 \overset{613\ K}{\rightarrow} Th(CO_3)_2 + 2CO$	
		$Th(CO_3)_2 \overset{663\ K}{\rightarrow} Th(OCO_3) + CO_2$	
		$Th(OCO_3) \overset{683\ K}{\rightarrow} ThO_2 + CO_2$	

3. Experimental

Thorium oxalate hexahydrate was precipitated by adding 0.5 M oxalic acid solution to 0.5 M thorium nitrate solution while stirring. The precipitate was digested for 1 h, filtered, washed and dried for 24 h at room temperature.

A Rheometric Scientific STA 1500 instrument was used for simultaneous TGA–DTA studies on this system. The sensitivity of the thermobalance in the range of operation was 1 μg. The temperature calibration was done by the method of fixed melting points by using ICTAC recommended standards like indium, tin and gold. Approximately 15 mg of thorium oxalate hexahydrate sample was taken for each experiment. Sintered high-density alumina crucibles were used as sample and reference holders, and α-alumina powder was used as reference material. Moist argon was used as ambient to ensure the starting compound as hexahydrate. Argon flowing through a leak tight container that held water at room temperature was used for this purpose and flow rate was maintained at 50 ml/min. Experiments were performed under non-isothermal conditions at programmed linear heating rates of 1, 2, 5 K/min. Experiments were carried out in duplicate and the agreement between them was excellent. TGA–DTA experiments were also performed with higher sample mass (85 mg) and at different heating rates (5 and 10 K/min) to simulate conditions used by earlier workers and compare the results. Experiments were also carried out in dry argon and in air at a heating rate of 5 K/min to study the effect of other ambients.

The starting compound and intermediate products were analysed by X-ray analysis by employing Siemens 800 X-ray diffractometer with Cu Kα radiation. With a view to characterise the intermediate products of decomposition, thermal runs of hexahydrate samples were interrupted in the TGA–DTA system (heating rate 5 K/min, cooling rate 60 K/min) at eight temperatures namely, 348, 473, 513, 583, 628, 643, 661, and 873 K and the products were analysed by XRD. Adequate care was taken to avoid moisture pick up before the XRD analysis.

The carbon analysis of intermediate products were carried out by oxidising the product into carbondioxide, and then estimating CO_2 quantitatively by using IR detector.

4. Results and discussion

XRD pattern of the starting compound is shown in Fig. 1 and confirms its stoichiometry as $Th(C_2O_4)_2{\cdot}6H_2O$ (JCPDS 22-1485). Fig. 2 shows the simultaneous TGA and DTA curves of thorium oxalate hexahydrate (solid and broken lines, respectively)

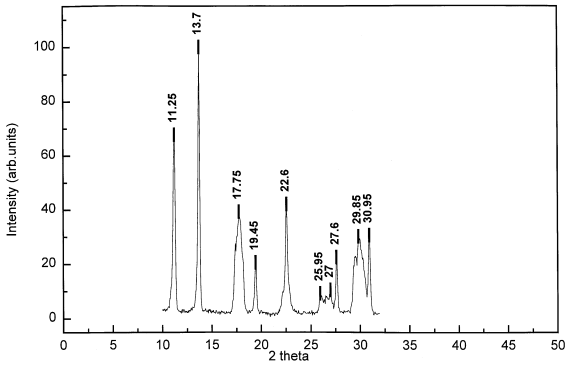

Fig. 1. XRD pattern of $Th(C_2O_4)_2{\cdot}6H_2O$ (JCPDS 22-1485).

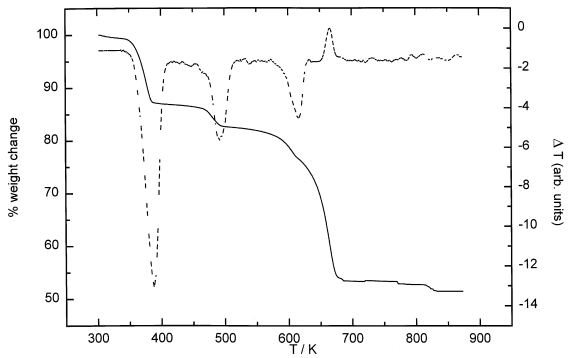

Fig. 2. TGA–DTA plots of decomposition of $Th(C_2O_4)_2{\cdot}6H_2O$ at 5 K/min in moist argon atmosphere (sample mass = 14 mg).

obtained at a heating rate of 5 K/min under moist argon atmosphere. The decomposition pattern obtained under other heating rates was similar except for the usual increase in the observed decomposition temperatures with increase in heating rate. The TGA and DTA curves under air and dry argon ambients are similar in pattern to that obtained in moist argon except special features at around 800 K. DTG results of experiments carried out under air and dry argon by using 15 mg of the sample is shown in Fig. 3 along with the results obtained in moist argon. The TGA–DTA pattern obtained with higher sample mass (85 mg) is shown in Fig. 4.

The first weight loss commencing at 350 K (Fig. 2) corresponds to the loss of four moles of water, and appears as an endothermic peak in the DTA curve. There is good agreement between the expected and observed weight loss for the loss of four moles of water as shown in Table 2. XRD pattern of the intermediate after heating up to 348 K and held at that temperature for 17 h is shown in Fig. 5(a). The pattern shows the product formed as thorium oxalate dihydrate (JCPDS 18-1365). The decomposition temperature obtained from 1 K/min heating rate was 343 K. This temperature obtained from the present work with low mass and low heating rate can

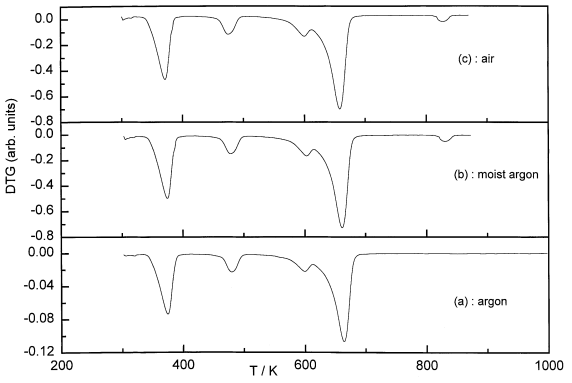

Fig. 3. DTG curve of $Th(C_2O_4)_2{\cdot}6H_2O$ in different atmospheres: (a) argon; (b) moist argon; (c) air; sample size: 15 mg; heating rate: 5 K/min.

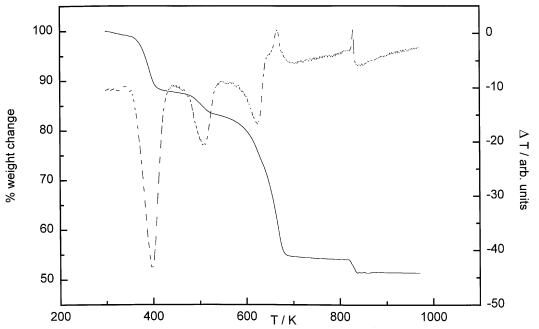

Fig. 4. TGA–DTA curve of $Th(C_2O_4)_2{\cdot}6H_2O$ in moist argon atmosphere; sample mass: 85 mg; heating rate: 5 K/min.

be taken as the decomposition temperature of hexahydrate of thorium oxalate to the dihydrate

$$Th(C_2O_4)_2 \cdot 6H_2O \overset{343\ K}{\rightarrow} Th(C_2O_4)_2 \cdot 2H_2O + 4H_2O \quad (1)$$

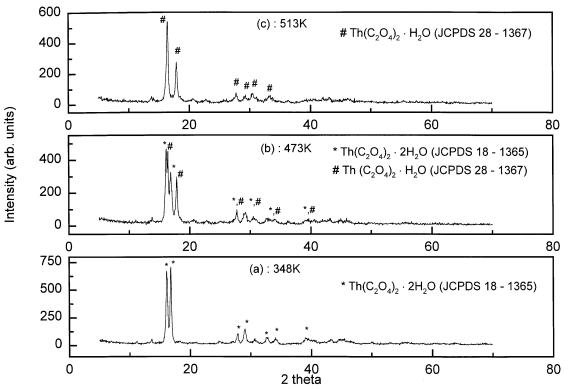

Fig. 5. XRD pattern of intermediates obtained at different temperatures: (a) 348 K; (b) 473 K; (c) 513 K.

This decomposition temperature derived from the work of Wendlandt et al. [3] is ~373 K (see Table 1). As seen from Table 1, Wendlandt et al. employed high-sample mass and heating rates. Our TGA–DTA results with similar conditions (85 mg, 10 K/min) showed the decomposition temperature to be 374 K.

The observed second mass loss step in Fig. 2 corresponds to loss of one mole of water yielding thorium oxalate monohydrate. The mass loss is also in good agreement with the expected value as represented in Table 2. Endothermic peak corresponding to this step is also seen in DTA curve. XRD pattern of the product formed after heating up to 473 K shows the presence of both dihydrate and monohydrate of thorium oxalate (Fig. 5(b)). The product obtained after heating up to 513 K was found to be only monohydrate (Fig. 5(c)). The dehydration temperature deduced from DTA results (heating rate = 1 K/min) is 453 K. Padmanabhan et al. [2] reported this dehydration temperature as 393 K which is lower by 60 K. Padmanabhan et al. reportedly prepared the starting oxalate by precipitating it from

Table 2
Comparison of the expected and observed weight loss for the decomposition of $Th(C_2O_4)_2 \cdot 6H_2O$ at 5 K/min in flowing moist argon atmosphere

Assumed reactions	Cumulative weight loss (%)	
	Expected	Observed
$Th(C_2O_4)_2 \cdot 6H_2O \rightarrow Th(C_2O_4)_2 \cdot 2H_2O + 4H_2O$	13.953	13.948
$Th(C_2O_4)_2 \cdot 2H_2O \rightarrow Th(C_2O_4)_2 \cdot H_2O + H_2O$	17.442	17.424
$Th(C_2O_4)_2 \cdot H_2O \rightarrow Th(C_2O_4)_2$	20.930	23.104[a]
$ThOCO_3 \rightarrow ThO_2 + CO_2$	48.837	47.233[b]
After carbon loss	48.837	48.539

[a] At temperature 615 K.
[b] Calculated from mass loss observed at 710 K.

aqueous thorium nitrate solution followed by drying over concentration H_2SO_4. This preparation is likely to result in formation of mixture of hydrates. Further, they had not characterised the starting compound by other instrumental techniques. Hence it is not appropriate to correlate mass loss obtained from the thermogravimetric analysis with exact stoichiometry of the intermediate product and also deduce decomposition temperatures. Wendlandt et al. [3] observed the dehydration of dihydrate to commence at 523 K. However, the authors deduced from the subsequent mass loss data that the anhydrous oxalate is formed directly from the dihydrate and not through the formation of the monohydrate. D'Eye and Sellman [1] also reported that the anhydrous oxalate is formed directly from the dihydrate based on their isothermal dehydration/decomposition studies. The temperature chosen for the isothermal heating in their work was 543 K, which is much higher than the temperature for the conversion of dihydrate to monohydrate. However, in both these works the intermediates were not structurally characterised. Thermogravimetric and X-ray analysis data of the present work clearly indicate that only thorium oxalate monohydrate is formed from the dihydrate and not the anhydrous salt. The reaction at this stage is represented as

$$\mathrm{Th(C_2O_4)_2 \cdot 2H_2O} \overset{453\ \mathrm{K}}{\rightarrow} \mathrm{Th(C_2O_4)_2 \cdot H_2O + H_2O} \qquad (2)$$

Fig. 2 shows that a third mass loss occurs between 570 and 635 K. From Table 2, it is seen that the observed weight loss in the third step is more than that expected when anhydrous thorium oxalate alone is assumed to be formed. XRD pattern of the intermediate obtained at 583 K is given in Fig. 6(a) and shows the presence of thorium oxalate monohydrate (JCPDS 28-1367) and anhydrous thorium oxalate (JCPDS 22-1478). In addition, broad peaks indicating the formation of an amorphous phase are observed in the 2θ range of 25–35° and 40–50°. XRD pattern of the intermediate obtained after heating the sample up to 628 K (Fig. 6(b)) shows only a mixture of anhydrous oxalate and the amorphous phase to be present. XRD pattern of the product obtained after heating the sample up to 643 K showed the presence of substantial quantities of the amorphous phase (Fig. 6(c)). These evidences indicate that thorium oxalate monohydrate decomposes to give two products, namely anhydrous oxalate and an amorphous compound within a narrow range of temperature. Consequently the mass loss associated in this stage cannot be correlated to fix the stoichiometry of the intermediate products. The amorphous phase could be a carbonate of thorium, as is reported in literature [1,5]. In order to prepare thorium carbonate independently, equimolar quantities of sodium carbonate and thorium nitrate solutions were mixed and treated. Thermogravimetric analysis of this compound was carried out by heating the sample up to 850°C whereupon the final product obtained was thorium oxide as confirmed by XRD. From the mass loss during this ignition to form the oxide, the stoichiometry was obtained as that of thorium oxycarbonate, $ThOCO_3$. Carbon analysis of the compound showed the carbon content to be 4.1% (theoretical value 3.9%) and thus confirming the stoichiometry as $ThOCO_3$. XRD pattern of this compound, shown in Fig. 7, indicates it to be amorphous in nature and this pattern closely resembles the pattern of the amorphous phase (Fig. 6(c)) obtained in TGA–DTA analysis. Formation of this oxycarbonate in addition to anhydrous oxalate leads to higher observed mass loss than expected by assuming the formation of anhydrous oxalate (Table 2). From the mass loss data, the amount of $ThOCO_3$ present at 615 K was found to be 11.2% and the remaining amount to be $Th(C_2O_4)_2$. The DTA curve in Fig. 2 shows the corresponding endotherm, which represents the resultant heat effect of these simultaneous processes. DTA curve obtained with 1 K/min indicates the process

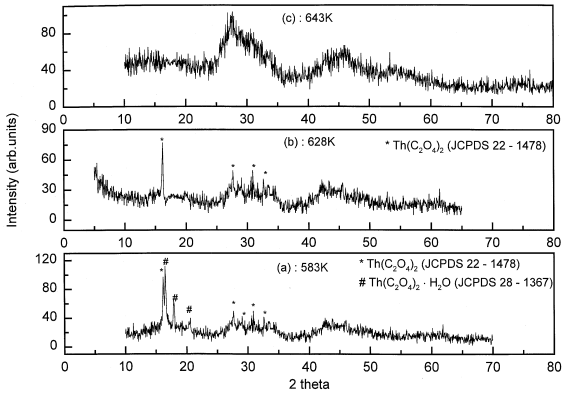

Fig. 6. XRD pattern of the intermediates obtained at different temperatures: (a) 583 K; (b) 628 K; (c) 643 K.

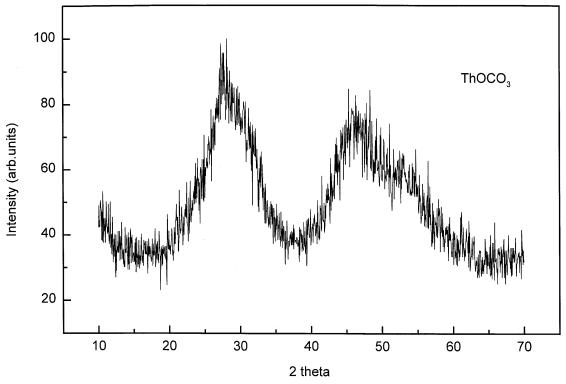

Fig. 7. XRD pattern of the prepared $ThOCO_3$.

to initiate at 570 K and extend up to 600 K. The processes that occur in this temperature range can be represented as

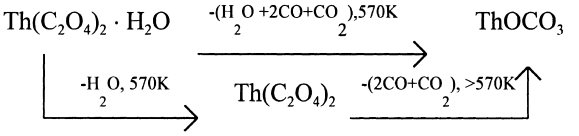

(3)

Fig. 2 shows that a substantial mass loss occurs in the temperature range of 635–675 K. While continuous weight loss is observed in TGA curve, significant heat effect was not observed in the temperature range 635–650 K in DTA curve. An exothermic peak is observed beyond this temperature range. XRD pattern of intermediate product obtained after heating the sample up to 661 K indicated the presence of thoria (Fig. 8(a)). XRD pattern of the product formed after heating up to 873 K shows the presence of well-crystalline thoria (Fig. 8(b)). Based on this X-ray data, the exothermic process can be attributed to decomposition of amorphous thorium oxycarbonate to yield thoria. The onset temperature for decomposition of $ThOCO_3$ deduced from the (exothermic) DTA peak that when sample heated at 1 K/min is 625 K, which is to be considered as the upper limit only. Although the endo and exo peaks are apparently well resolved it is not appropriate to deduce onset temperature for decomposition of $ThOCO_3$ from the exothermic peak alone since endo and exothermic processes occur simultaneously in the temperature range of relevance. The fourth stage is represented as

$$ThOCO_3 \rightarrow ThO_2 + CO_2 \quad (4)$$

Since the reaction temperature for the formation of intermediates and final product are very close, a clear separation of steps is not observed in the TGA curve

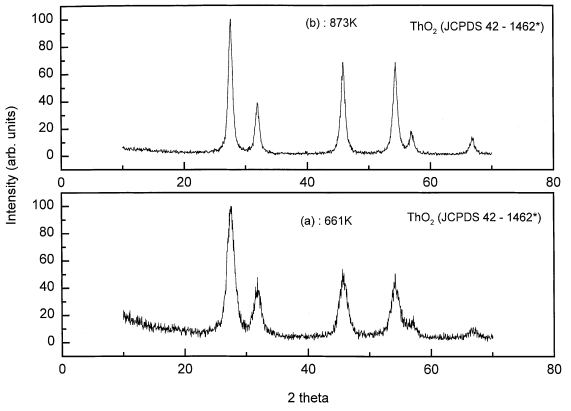

Fig. 8. XRD data of the product obtained at: (a) 661 K and (b) 873 K.

between third and fourth mass loss steps. A comparison of total weight loss from thorium oxalate hexahydrate to thoria was evaluated at 710 K and is shown in Table 2. This shows that the observed weight loss is less than that of the expected value. Since free carbon is known to be formed during low temperature ignition of thorium oxalate to thoria [1,6], products formed by heating the sample up to 773 and 823 K were analysed for their carbon contents and were found to be 2.502% and 60 ppm, respectively. The presence of free carbon in the product results in the lower than expected mass loss in the temperature range considered. The presence of free carbon in the product is also shown by the small but definite mass loss in TGA curve above 800 K. This is distinctly seen in the TGA–DTA curve with high-mass sample in moist argon ambient (Fig. 4). An additional exothermic DTA peak observed in this high-mass experiment corresponds to the ignition of free carbon to carbondioxide. DTG curve of the thorium oxalate hexahydrate under dry argon ambient was carried out (Fig. 3) and this does not show the mass loss in this temperature range hereby confirming the conclusions arrived at.

From all these discussions, the scheme of decomposition of thorium oxalate hexahydrate to form thoria can be summarised as follows:

$$Th(C_2O_4)_2 \cdot 6H_2O \xrightarrow{343\ K} Th(C_2O_4)_2 \cdot 2H_2O + 4H_2O, \quad (1)$$

$$Th(C_2O_4)_2 \cdot 2H_2O \xrightarrow{453\ K} Th(C_2O_4)_2 \cdot H_2O + H_2O, \quad (2)$$

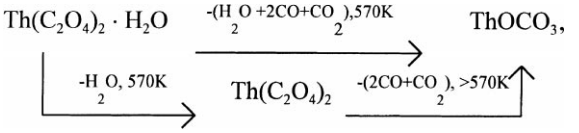

(3)

$$ThOCO_3 \rightarrow ThO_2 + CO_2. \quad (4)$$

It is to be pointed out that Aybers proposed formation of $Th(CO_3)_2$ and $ThOCO_3$ as intermediate products in the decomposition sequence and this was based on DTA and surface area measurements. Aybers observed two close and unresolved exothermic peaks in the temperature range of ca. 573–683 K and this was attributed to formation of $Th(CO_3)_2$ from $Th(C_2O_4)_2$ followed by formation of $ThOCO_3$. Increase in surface area (due to evolution of gas and formation of pores) during formation of intermediates followed by decrease in surface area (due to sintering) after the intermediate was formed was also taken as supporting evidence. In the present work, DTA results with high-sample mass and with low heating rate (1 K/min) did not show double exothermic peak in the temperature region of relevance. Based on the DTA and XRD studies, it is evident that the

intermediate product formed is $ThOCO_3$. The increase in surface area observed by Aybers may be due to the loss of free carbon. The dispersed carbon on reaction with moisture or O_2 releases CO_2. The evolution of CO_2 increases the probability of pore formation during the course of the reaction. Increase in porosity would increase the surface area of the resultant powder. Further increase in temperature would cause sintering, thus reduce the surface area of the powder.

5. Dissociation mechanism and kinetic parameters

Kinetic analysis of the thermal data obtained for all the stages of decomposition was done in order to arrive at the mechanism of dissociation processes and to deduce the kinetic parameters. Kinetic parameters can be obtained employing either a physical model dependent method or a physical model independent method. The former method is found to be better one compared to that of the physical model independent method [7] because the latter method employs very generalised rate expression and cannot predict the mechanism of the process. In the present study, kinetic parameters were evaluated employing physical model dependent method.

The rate of the reaction under nonisothermal condition can be expressed by the following relation [8]:

$$\frac{d\alpha}{dT} = \frac{k(T)}{\beta} f(\alpha), \tag{5}$$

where α is the fraction reacted at temperature T, $f(\alpha)$ the conversion function which is dependent on the mechanism of the reaction, β the rate of heating employed in the experiment and $k(T)$ is the rate constant as a function of temperature. Eq. (5) can be represented by its integral form as follows:

$$g(\alpha) \equiv \int_0^{\alpha} \frac{d\alpha}{f(\alpha)} = \int_0^{T} \left(\frac{A}{\beta}\right) \exp\left[\frac{-E}{RT}\right] dT, \tag{6}$$

where A is the pre-exponential factor, E the activation energy and R is the gas constant. The algebraic expression of the integral $g(\alpha)$ functions that are tested in this work are listed in Table 3. These expressions are applied for the kinetic analysis of solid state reactions and encompass most common mechanisms.

Both TGA and DTA experimental data were used to evaluate kinetic parameters and arrive at the mechanism of the reaction of the first two steps. For the third and fourth steps, kinetic parameters were evaluated using only DTA data. This is because of the difficulty in resolving these two steps in the TGA curve. From the mass loss and DTA experiments, α, the fraction reacted was evaluated as a function of temperature. A typical plot of α versus temperature for stage 1 is shown in Fig. 9. Similar plots were made for other stages also. The α range of 0.10–0.92 were used for the kinetic analysis of the first and second stages and a range of 0.16–0.88 were utilised for the third and fourth steps. The kinetics of the different stages of the thermal decomposition of thorium oxalate hexahydrate was followed by employing the Coats and Redfern approximation [9] which gives the expression

$$\ln\left[\frac{g(\alpha)}{T^2}\right] = \ln\left[\frac{AR}{\beta E}\left(1 - \frac{2RT}{E}\right)\right] - \frac{E}{RT}. \tag{7}$$

A plot of $\ln(g(\alpha)/T^2)$ versus $1/T$ gives a straight line when the correct $g(\alpha)$ function is used in the equation. The $g(\alpha)$ function describes the mechanism of the reaction. Straight lines with high-correlation coefficient and low standard deviation were selected to represent the possible controlling mechanism. The corresponding kinetic parameters were then calculated and are shown in

Table 3
List of solid state rate equations used in the present study

Rate controlling mechanism	$g(\alpha)$
P1 power law	$\alpha^{1/n}$
E1 exponential law	$\ln\alpha$
A2 Avrami–Erofe'ev equation 1	$[-\ln(1-\alpha)]^{1/2}$
A3 Avrami–Erofe'ev equation 2	$[-\ln(1-\alpha)]^{1/3}$
A4 Avrami–Erofe'ev equation 3	$[-\ln(1-\alpha)]^{1/4}$
B1 Prout–Tompkins	$\ln[\alpha/(1-\alpha)]$
R2 contracting area	$1-(1-\alpha)^{1/2}$
R3 contracting volume	$1-(1-\alpha)^{1/3}$
D1 one-dimensional diffusion	α^2
D2 two-dimensional diffusion	$(1-\alpha)\ln(1-\alpha)+\alpha$
D3 three-dimensional diffusion, Jander's	$[1-(1-\alpha)^{1/3}]^2$
D4 three-dimensional diffusion, Ginstling Brounshtein	$(1-2\alpha/3)-(1-\alpha)^{2/3}$
F1 first order	$-\ln(1-\alpha)$
F2 second order	$1/(1-\alpha)$
F3 third order	$[1/(1-\alpha)]^2$

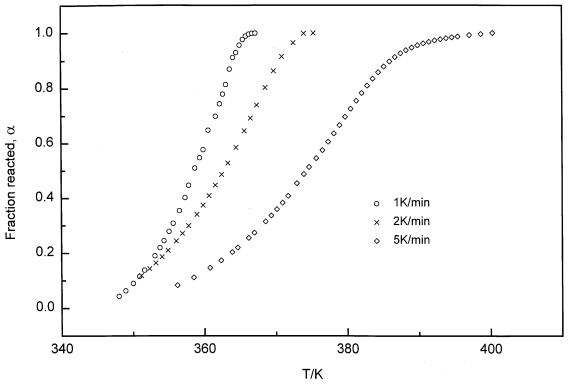

Fig. 9. Plot of fraction reacted $g(\alpha)$ versus temperature for the stage 1.

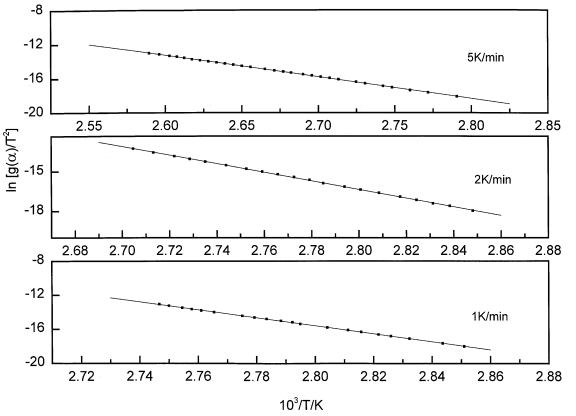

Fig. 10. Plot of $[g(\alpha)/T^2]$ versus $1/T$ for stage 1 using DTA data; $g(\alpha) = [1-(1-\alpha)^{1/3}]^2$.

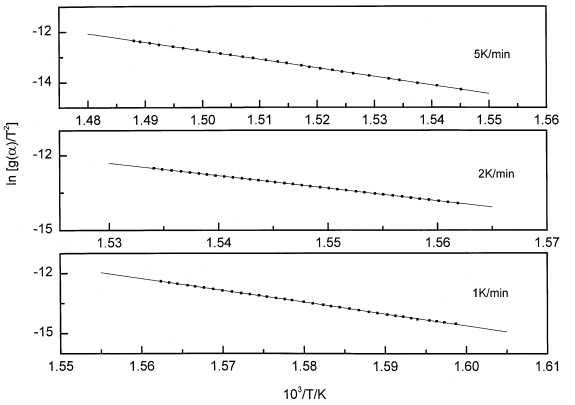

Fig. 11. Plot of $[g(\alpha)/T^2]$ versus $1/T$ for stage 4 using DTA data; $g(\alpha) = [-\ln(1-\alpha)]^{1/2}$.

Table 4. The best fit for the first and second dehydration steps of $Th(C_2O_4)_2{\cdot}6H_2O$ is obtained using D3, Janders diffusion model. The third step also gives best fit with Jander's D3 diffusion model. The activation energy obtained for the third step was found to be much higher than the values obtained for the earlier dehydration steps. This is attributed to the occurrence of simultaneous reactions mentioned earlier in the temperature range of relevance. For the fourth step, best fit was obtained with A2, two-dimensional Avrami–Erofe'ev model which corresponds to nucleation and growth mechanism. Plots of $\ln(g(\alpha)/T^2)$ versus $1/T$ for the first and fourth decomposition step are shown in Figs. 10–12. Theoretically the activation energy of a process is expected not to change with change in heating rate. But the activation energy is found to decrease with increase in heating rate and this has been reported in literature, for e.g. [10–12]. Similarly pre-exponential factor was also found to change with heating rate. The real activation energy for each decomposition step would be the one obtained under lowest heating rate. The kinetic parameters obtained from TGA and DTA data are in good agreement.

Table 4
Kinetic parameters and possible rate controlling processes of decomposition of $Th(C_2O_4)_2 \cdot 6H_2O$ (nonisothermal conditions)

	Mech	β (K/min)	E (kJ/mol)		$\log A$/min	
			DTA	TGA	DTA	TGA
Stage 1	D3	1	391 ± 2	399 ± 2	55.1 ± 4.9	56.2 ± 1.9
		2	270 ± 1	260 ± 1	37.2 ± 4.9	36.0 ± 4.9
		5	210 ± 1	198 ± 1	27.8 ± 5.2	26.3 ± 5.2
Stage 2	D3	1	413 ± 3	412 ± 2	41.2 ± 5.0	43.8 ± 4.8
		2	351 ± 1	367 ± 2	33.9 ± 5.0	38.9 ± 5.1
		5	278 ± 3	284 ± 2	28.4 ± 5.5	29.4 ± 5.4
Stage 3	D3	1	872 ± 6	–	75.4 ± 5.5	–
		2	816 ± 6	–	71.6 ± 5.4	–
		5	711 ± 3	–	60.8 ± 5.8	–
Stage 4	A2	1	492 ± 2	–	39.5 ± 4.8	–
		2	417 ± 1	–	33.0 ± 5.0	–
		5	282 ± 1	–	21.8 ± 5.3	–

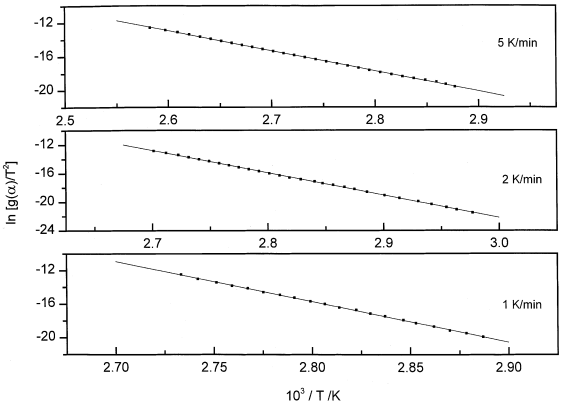

Fig. 12. Plot of $[g(\alpha)/T^2]$ versus $1/T$ for stage 1 using TGA data $g(\alpha) = [1-(1-\alpha)^{1/3}]^2$.

In order to validate the reaction mechanism deduced from non-isothermal experiments and the evaluated kinetic parameters, isothermal experiments were carried out at different temperatures in each decomposition step. From the mass loss measured, the fraction reacted (α) was evaluated as a function of time. A typical α versus time plot is shown for stage 1 in Fig. 13. Similar plots were made for other stages also. The integral form of the isothermal kinetic equation is represented as

$$g(\alpha) = kt, \tag{8}$$

where k is the rate constant at the chosen temperature and t is the time. As in non-isothermal experiments, best fit for first three stages is obtained only with D3 Janders three-dimensional diffusion model. Diffusion mechanism suggests that evolved species (like H_2O, CO_2, CO) are accommodated within the channels of the lattice from which it escapes [13]. The Avrami–Erofe'ev A2 nucleation and growth model gives the best fit for the formation of thoria in the fourth stage as observed in non-isothermal kinetics. The values of the rate constant and the corresponding temperatures are listed in Table 5. Using Arrhenius equation, the activation energy, E, and pre-exponential factor, A, for each process was evaluated and shown in Table 6. The Arrhenius plot for different stages are shown in Fig. 14. The activation

Table 5
Values of the rate constants as a function of temperature for each decomposition stage

	Mechanism	T/K	Rate constant (k/min)
Stage 1	D3	343	3.230×10^{-4}
		348	2.440×10^{-3}
		353	1.319×10^{-2}
		358	1.030×10^{-1}
Stage 2	D3	458	7.780×10^{-3}
		463	2.751×10^{-2}
		468	6.414×10^{-2}
		473	2.520×10^{-1}
Stage 3	D3	543	1.205×10^{-6}
		553	6.611×10^{-5}
		568	4.430×10^{-3}
		573	2.858×10^{-2}
		578	9.405×10^{-2}
Stage 4	A2	618	2.453×10^{-2}
		628	7.368×10^{-2}
		638	3.607×10^{-1}
		643	5.596×10^{-1}

Table 6
Calculated activation energy (E) and pre-exponential factor (A) under isothermal conditions

	Mechanism	Activation energy E (kJ/mol)	Pre-exponential factor $\log A$ (min)
Stage 1	D3	387 ± 11	55.5 ± 1.6
Stage 2	D3	406 ± 25	44.2 ± 2.8
Stage 3	D3	828 ± 29	74.1 ± 2.6
Stage 4	A2	428 ± 28	34.5 ± 2.3

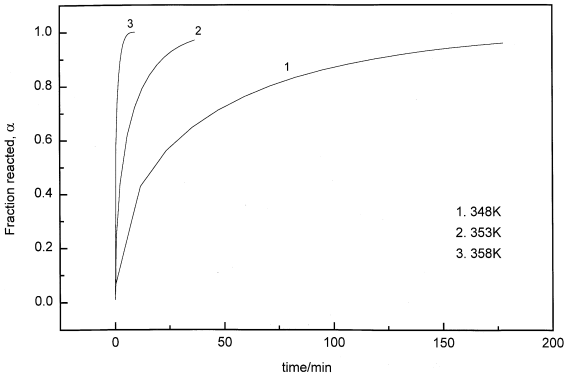

Fig. 13. Plot of fraction reacted $g(\alpha)$ versus time at different isothermal conditions for the stage1.

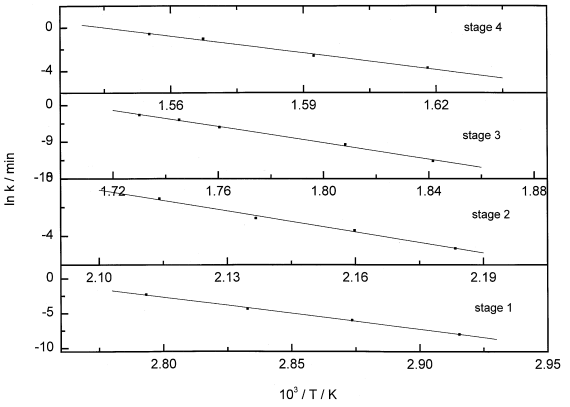

Fig. 14. Arrhenius plot of different stages.

energies derived from both nonisothermal experiments at the lowest heating rate, and isothermal conditions were found to be in good agreement with each other and this confirms the validity of the reaction mechanism deduced for each stage.

6. Conclusions

The thermal decomposition of thorium oxalate hexahydrate occurs in four steps. The first and second dehydrations occur at 343 and 453 K. This dehydration is governed by D3 Janders diffusion mechanism. In the temperature range of 570–600 K, the third dehydration and further decomposition to form thorium oxycarbonate occur. The above step also corresponds to D3 diffusion mechanism. The fourth step corresponds to formation of thoria from amorphous thorium oxycarbonate. Kinetic parameters were deduced at each stage under both nonisothermal and isothermal conditions. The kinetic parameters obtained from isothermal experiments are in good agreement with those of the nonisothermal experiments carried out at the lowest heating rate.

Acknowledgements

The authors thank Dr K.V.G. Kutty and Shri H.N. Jena for their help in obtaining X-ray diffractograms. The authors also thank Dr V. Chandramouli for his help in obtaining carbon analysis of the samples. The authors also thank Dr K.S. Viswanathan for his fruitful suggestions. We are grateful to Dr G. Periaswami, Head, Materials Chemistry Division, for his constant encouragement during the course of the present investigations.

References

[1] R.W.M. D'Eye, P.G. Sellman, J. Inorg. Nucl. Chem. 1 (1955) 143.
[2] V.M. Padmanabhan, S. Saraiya, A.K. Sundaram, J. Inorg. Nucl. Chem. 12 (1960) 356.
[3] W.W. Wendlandt, T.D. George, G.R. Horton, J. Inorg. Nucl. Chem. 17 (1961) 273.
[4] M.S. Subramanian, R.N. Singh, H.D. Sharma, J. Inorg. Nucl. Chem. 31 (1969) 3789.
[5] M.T. Aybers, J. Nucl. Mater. 252 (1998) 28.
[6] P. Balakrishna, B.P. Varma, T.S. Krishnan, T.R.R. Mohan, P. Ramakrishnan, J. Nucl. Mater. 160 (1988) 88.
[7] A.M. Gadalla, Thermochim. Acta 95 (1985) 179.
[8] M.E. Brown, D. Dollimore, A.K. Galwey, Comprehensive Chemical Kinetics, vol. 22, Elsevier, Amsterdam, 1988.
[9] A.N. Coats, J.P. Redfern, Nature 201 (1964) 68.
[10] P.K. Heda, D. Dollimore, K.S. Alexander, Dun Chen, E. Law, P. Bicknell, Thermochim. Acta 255 (1995) 255.
[11] E. Urbanovici, E. Segal, Thermochim. Acta 107 (1986) 359.
[12] S.B. Kanungo, S.K. Mishra, Thermochim. Acta 241 (1994) 171.
[13] Y. Suzuki, Thermochim. Acta 255 (1995) 155.